SAND2016-6286C

$CaMnO_3$-based Materials for CSP Thermochemical Energy Storage

Andrea Ambrosini
Sandia National Labs

Sean Babiniec, Eric Coker, Peter Loutzenhiser, James E. Miller

ASME PowerEnergy 2016
Session 2-5-2: Thermal and Thermochemical Energy Storage – I
27 June 2015

Acknowledgements

- Peter Loutzenhiser (Georgia Tech)
- Shannon McKean (USNA)
- Ellen Stechel (Arizona State)
- The PROMOTES Team
- Bonnie McKenzie (Sandia)
- Mark Rodriguez (Sandia)
- Travis Anderson (Sandia)
- National Solar Thermal Test Facility at Sandia National Labs

Sandia National Laboratories is a multi-program laboratory managed and operated by Sandia Corporation, a wholly owned subsidiary of Lockheed Martin Corporation, for the U.S. Department of Energy's National Nuclear Security Administration under contract DE-AC04-94AL85000. This material is based upon work supported by the U.S. Department of Energy SunShot Initiative under Award Number DE-FOA-0000805.

PROMOTES

High Performance Reduction/Oxidation Metal Oxides for Thermochemical Energy Storage

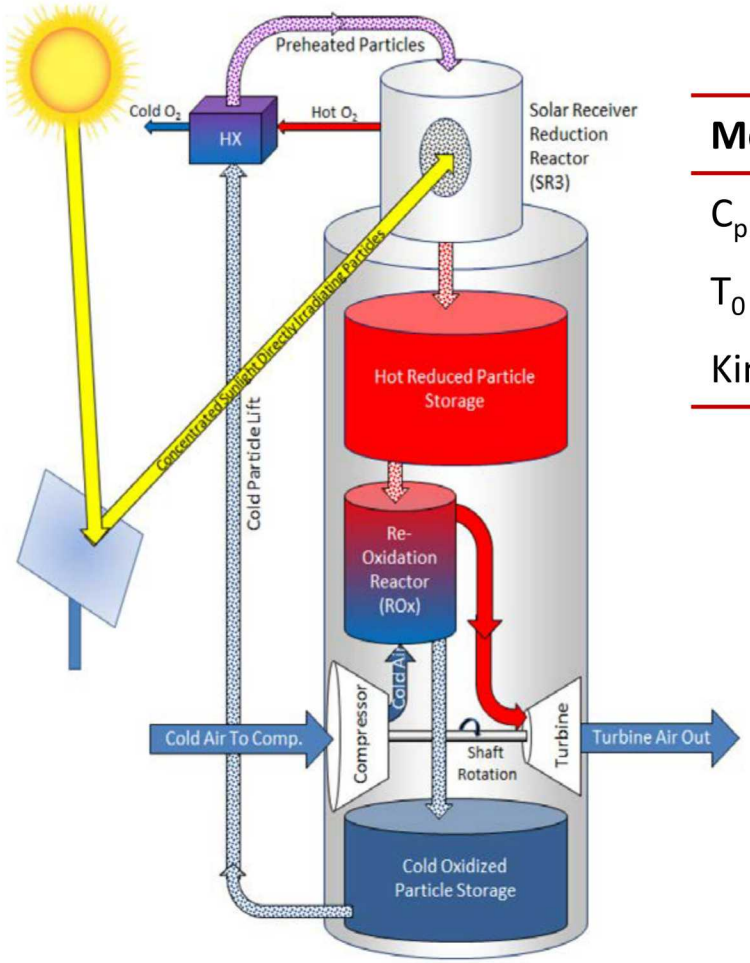

SunShot Goals

Metric	Goal	Metric	Goal
C_p	0.6 kJ/kg*K	ΔH_{total}	> 1500 kJ/kg
T_0	1000-1200 °C	δ (realized)	$0.2 < \delta < 0.5$
Kinetics	> $8x10^{-4}$ mol O_2/s	System Cost	< \$15/kWh_t

Parameter Space:

- Energy storage capacity, $\Delta H_{tot} = \Delta H_{rxn} + C_p \Delta T$ =1500 kJ/kg
- Cycling between T_H of 1000 – 1350 °C and T_L of 200 °C
- pO_2 during reduction ≥ 10^{-3} atm
- pO_2 during oxidation ≤ 1 atm
- Oxygen non-stoichiometry (δ) = 0.2 – 0.5

KEY PARTNERS: Georgia Institute of Technology, King Saud University, Arizona State University

Mixed Ionic-Conducting (MIEC) Oxides

- Redox-active materials which efficiently conduct both O^{2-} and electrons
- No crystallographic phase change occurs during redox
- Vacancies facilitate oxide ion transport
- Redox activity continuous over variety of T and pO2

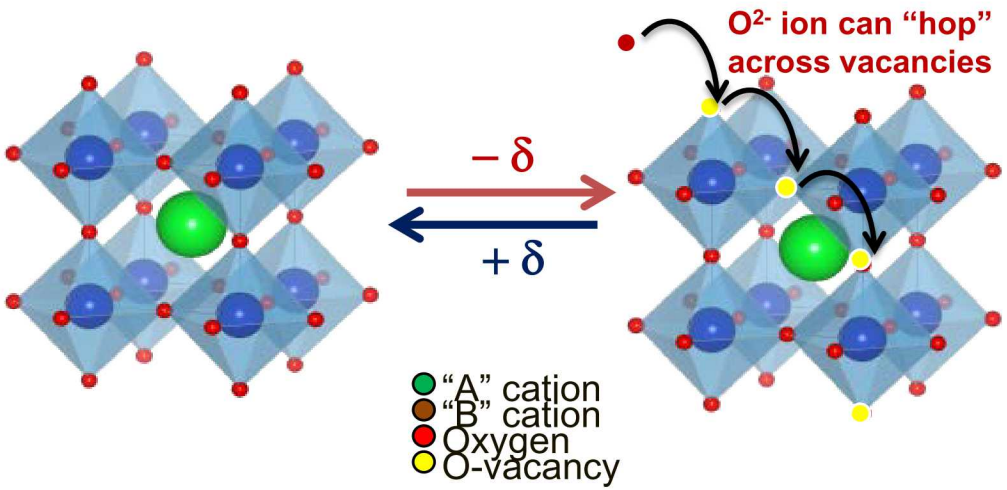

Advantages of Metal Oxides (MO):

- Open or closed configurations
- Air can act as both the reactant and heat transfer fluid
- Environmentally benign
- No catalyst necessary
- No compression required for storage
- Amenable to multiple scales and temperature ranges

Doped $LaCoO_3$

$La_xSr_{1-x}Co_yMn_{1-y}O_{3-\delta}$ (LSCM) and $La_xSr_{1-x}Co_yFe_{1-y}$ (LSCF)

- Known redox-active perovskite materials
- Large solid solubility range
- Crystallize in several perovskite-related space groups
- In general: more symmetric space groups show higher redox capacities

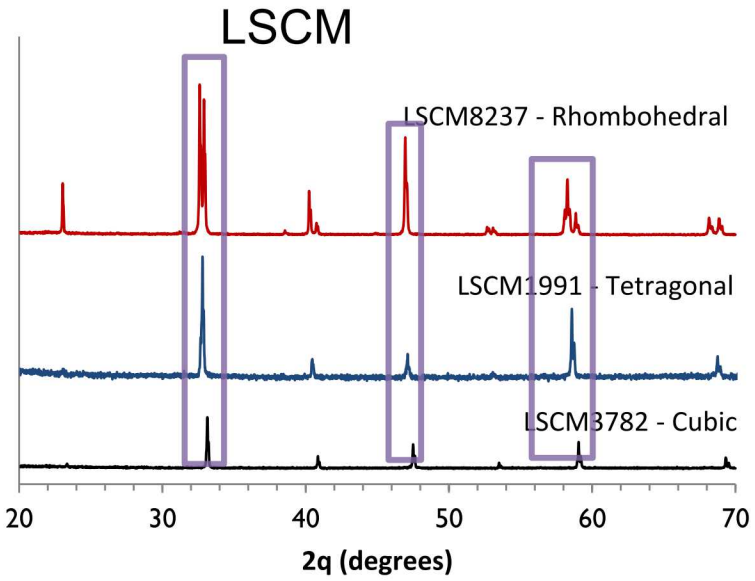

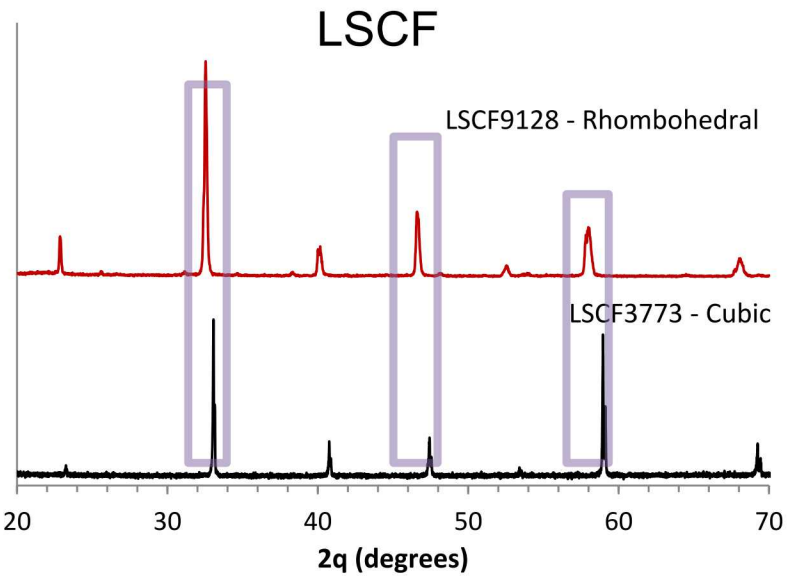

LSCM/LSCF Compositions

$La_xSr_{1-x}Co_yFe_{1-y}O_{3-\delta}$ ("LSCFXXXX")

Material Composition	Crystallographic Phase	Reduction Onset (°C)	Reoxidation Δδ
LSCM1991	Tetragonal	432	0.32
LSCM1982	Tetragonal	438	0.31
LSCM1973	Tetragonal	431	0.28
LSCM2891	Tetragonal	425	0.33
LSCM2882	Tetragonal	256	0.28
LSCM2873	Tetragonal	395	0.31
LSCM3791	Cubic	343	0.39
LSCM3782	Cubic	359	0.36
LSCM3773	Cubic	358	0.31
LSCM4664	Cubic	334	0.24
LSCM7337	Rhombohedral	772	0.01
LSCM8228	Rhombohedral	932	-0.01
LSCM8237	Rhombohedral	972	0.00
LSCM9119	Orthorhombic	825	0.02
LSCM9128	Orthorhombic	834	0.00
LSCM9137	Orthorhombic	901	-0.01

$La_xSr_{1-x}Co_yMn_{1-y}O_{3-\delta}$ ("LSCMXXXX")

Material Composition	Crystallographic Phase	Reduction Onset (°C)	Reoxidation Δδ
LSCF1991	Cubic	406	0.31
LSCF1982	Cubic	394	0.37
LSCF1973	Cubic	372	0.36
LSCF2891	Cubic	369	0.38
LSCF2882	Cubic	357	0.38
LSCF2873	Cubic	366	0.38
LSCF2828	Cubic	340	0.35
LSCF3791	Cubic	352	0.38
LSCF3773	Cubic	348	0.40
LSCF4691	Cubic	342	0.35
LSCF4682	Cubic	332	0.36
LSCF4673	Cubic	336	0.35
LSCF4646	Cubic	349	0.30
LSCF4664	Rhombohedral	342	0.32
LSCF5555	Rhombohedral	500	0.29
LSCF6446	Rhombohedral	609	0.22
LSCF7337	Rhombohedral	736	0.19
LSCF8228	Rhombohedral	926	0.06
LSCF8237	Rhombohedral	886	0.08
LSCF9128	Rhombohedral	1005	0.01
LSCF9137	Rhombohedral	970	0.03

Materials with highest oxygen capacity (δ) advanced to equilibrium TGA measurements

High-Resolution Equilibrium TGA

- Used to estimate thermodynamic parameters
- Isothermal holds at 600, 800, 950, 1100, and 1250 °C; pO_2 varied at each temperature and held until equilibrium
- Thermodynamic parameters extracted by van't Hoff approach:

$$\ln(pO_2) = 2\frac{-\Delta G_{rxn}}{RT} = 2\left(\frac{1}{T}\cdot\frac{-\Delta H_{rxn}}{R} + \frac{\Delta S_{rxn}}{R}\right)$$

- Enthalpy determined by slope, entropy by intercept for each value of δ

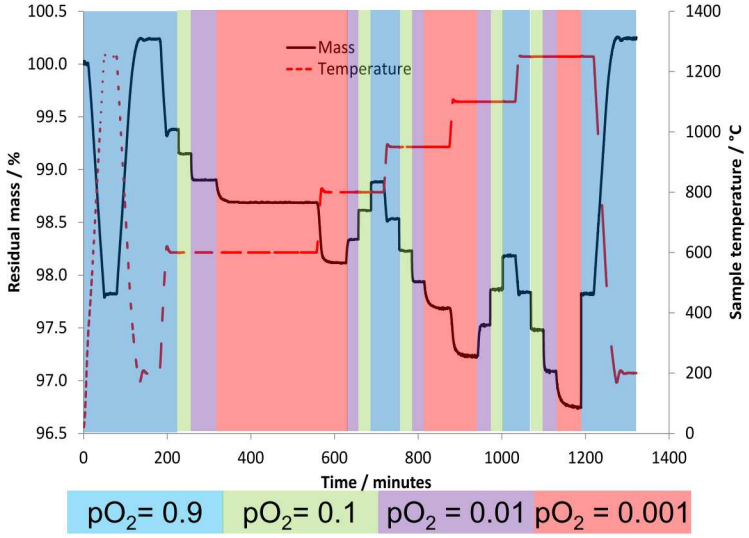

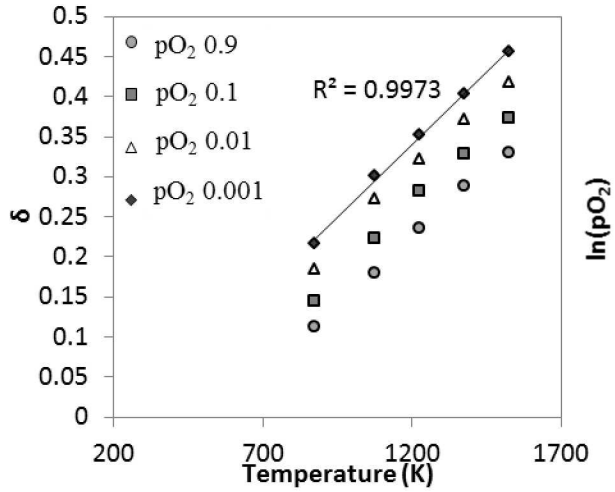

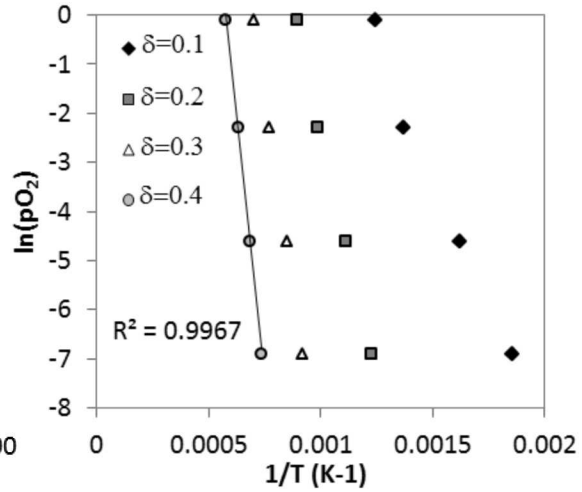

LSXM Enthalpy

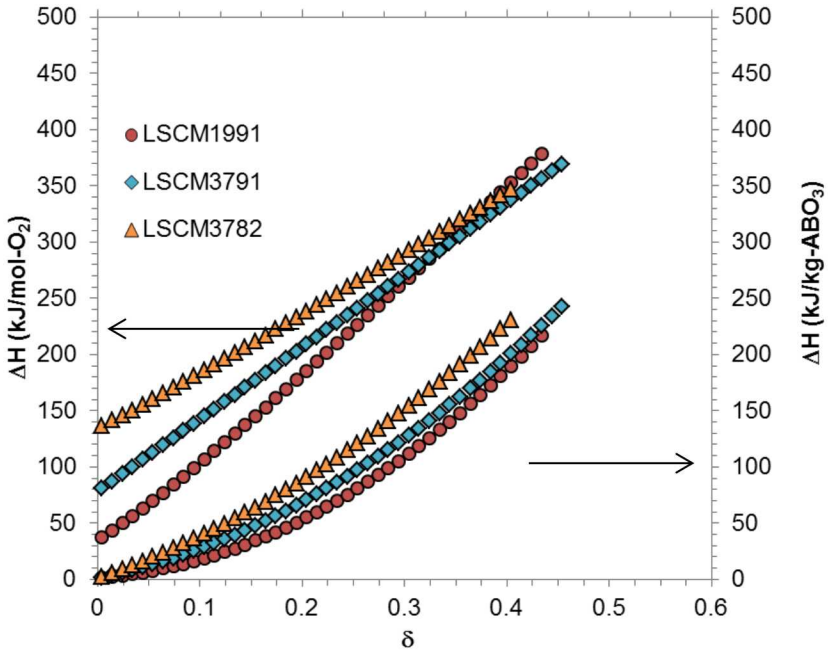

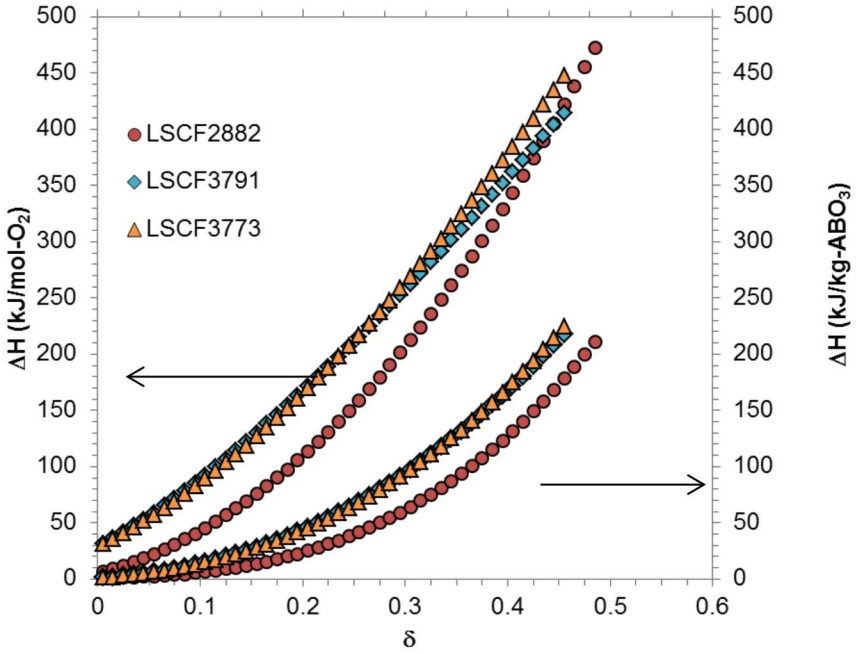

Material	Reduction onset (°C)	Maximum δ	Enthalpy at δ_{max} (kJ/kg)
LSCM1991	432	0.434	216
LSCM3791	343	0.460	242
LSCM3782	359	0.412	236
LSCF2882	357	0.486	212
LSCF3791	352	0.461	223
LSCF3773	348	0.455	223

LSCX Summary

- The $La_xSr_{1-x}Co_yX_{1-y}O_{3-\delta}$ (X = Mn,Fe) perovskites display many of the required characteristics required for high temperature TCES
  - Redox active
  - Reduction > $\Delta\delta = 0.35$ observed for several compositions
  - Do not degrade when cycled
  - Stable in operating environment
- Studies provided insight on structural/thermal properties of TCES perovskites
- However, LSCM/LSCF are not optimal
  - Reduction extent is adequate, but enthalpy falls short of SunShot goal (1500 kJ/kg)
  - Constituent oxides are not earth abundant

Increasing Reaction Enthalpy

- $\Delta G_{red} = \Delta H_{red} - T\Delta S_{red}$,
- $\Delta G_{red} = 0$ is the onset of reduction (equilibrium)
  - Assuming entropy term is similar between materials (i.e., constant), a change in reduction enthalpy necessitates a change in reduction temperature

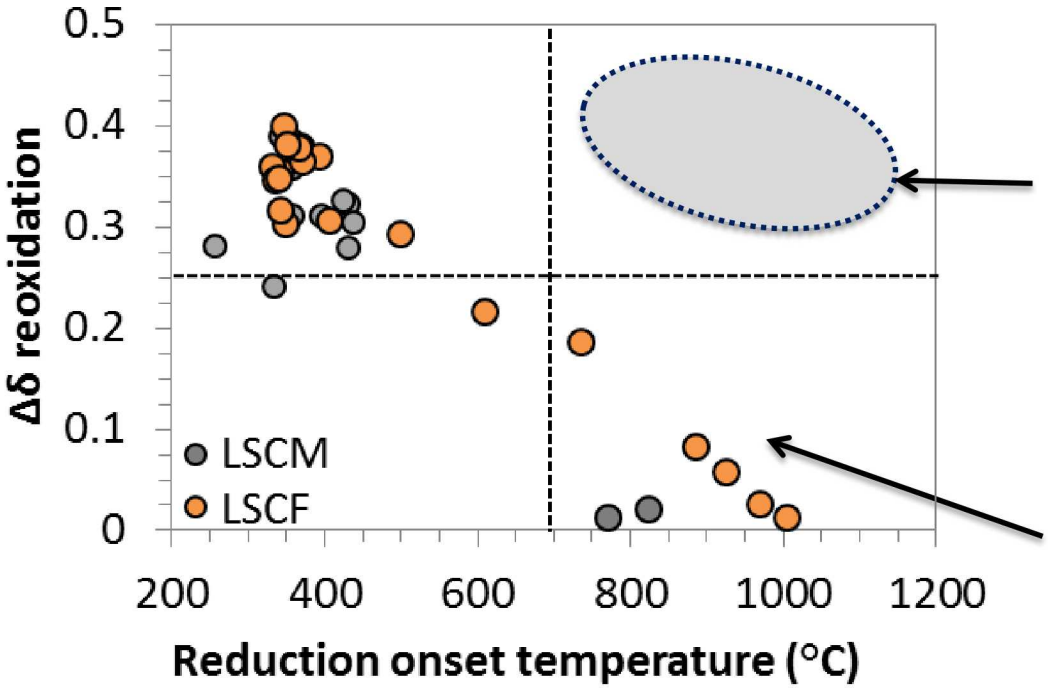

Ideal materials show a favorable balance of increased reduction onset temperature without large decrease in reduction capacity. New compositions focus on materials in this window.

In the LSCX system, materials with high reduction temperatures had low redox capacity ($\delta < 0.25$).

Doped $CaMn_{1-y}B_yO_{3-\delta}$ Perovskites

- Ca is a +2 element, forcing the B-site, e.g. Mn, to adopt a higher oxidation state (+4)
- Ca as the main element in the A-site lowers the molecular weight dramatically (Ca = 40.078 g/mol)
- Ca more abundant and less expensive than Sr or La
- Calcium perovskites reduce at high temperatures, resulting in increased partial molar reduction enthalpies
  - Higher reduction temperatures indicative of stronger M-O bonds
- T_{red} of $CaMnO_3$ = 875 °C (vs. 432 °C for LSCM1991)
  - However, decomposes under reducing conditions
  - Doping CMO can help stabilize the structure

Stability Under Reducing Conditions

- CCM28 and CM decompose under 1000 ºC Ar anneal
- CTM28 and CAM28 convert from orthorhombic (blue) to tetragonal (red)

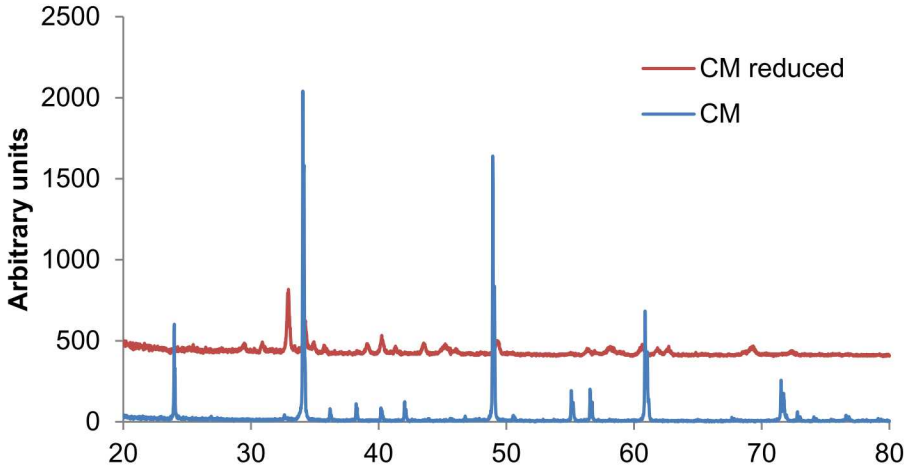

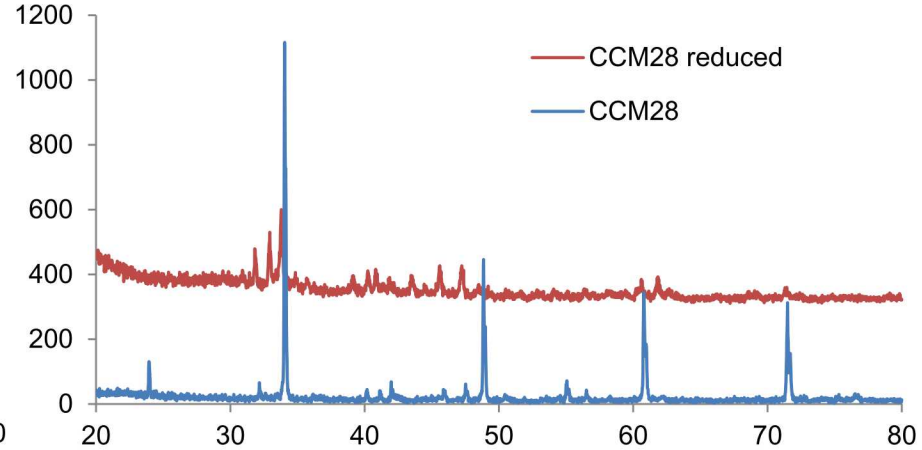

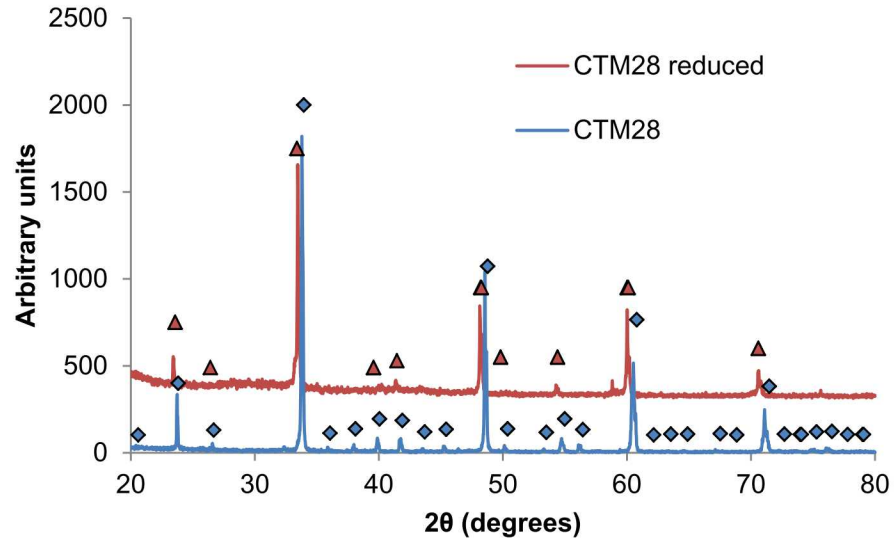

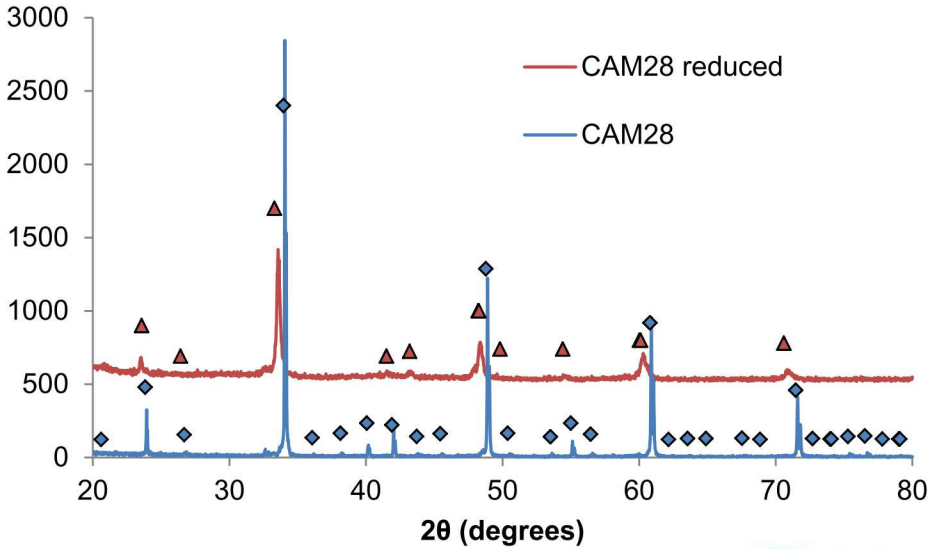

CAM28 In-situ XRD

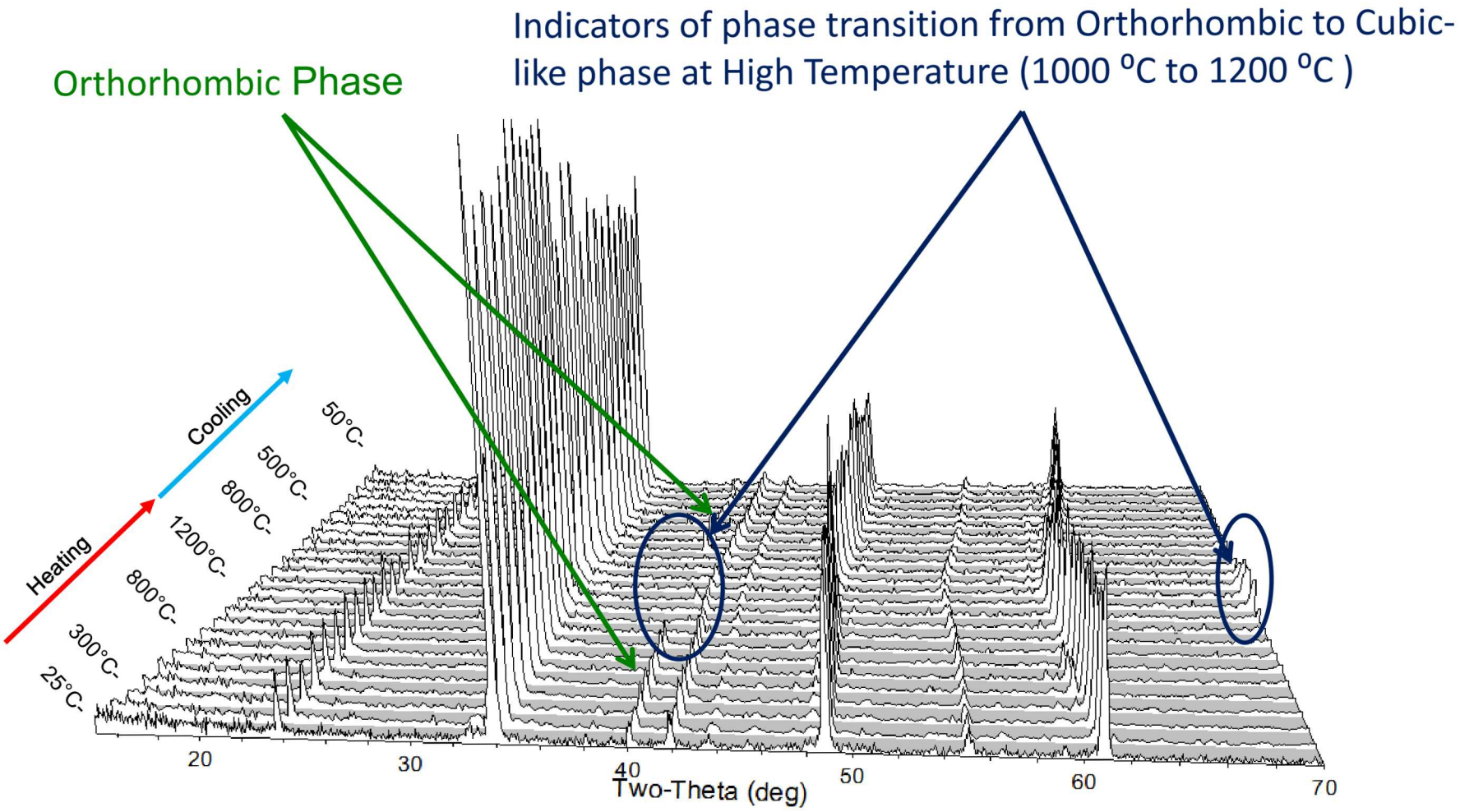

HT XRD results for: **Cam28 low_pO2**

Total storage potential

$$\Delta H_{tot} = \Delta H_{rxn} + C_p \Delta T$$

Latent heat assumes pO_2 swing of 0.001 to 0.9
Sensible heat assumes $C_p = 15R, T_L = 200\ °C$

LSCM3791

Temperature (°C)	Sensible (kJ/kg)	Latent (kJ/kg)	Total (kJ/kg)
1100	536	192	728
1200	595	225	820
1350*	684	289*	973

CTM28

Temperature (°C)	Sensible (kJ/kg)	Latent (kJ/kg)	Total (kJ/kg)
1100	793	290	1083
1200	881	362	1243
1350*	1013	481*	1494

CAM28

Temperature (°C)	Sensible (kJ/kg)	Latent (kJ/kg)	Total (kJ/kg)
1100	826	293	1119
1200	918	351	1269
1350*	1056	450*	1506

*Values at 1350 °C are extrapolated from δ vs T data

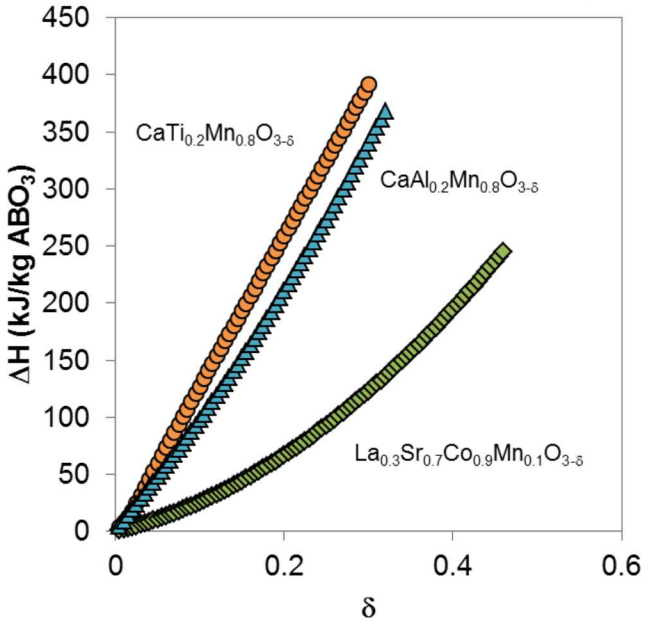

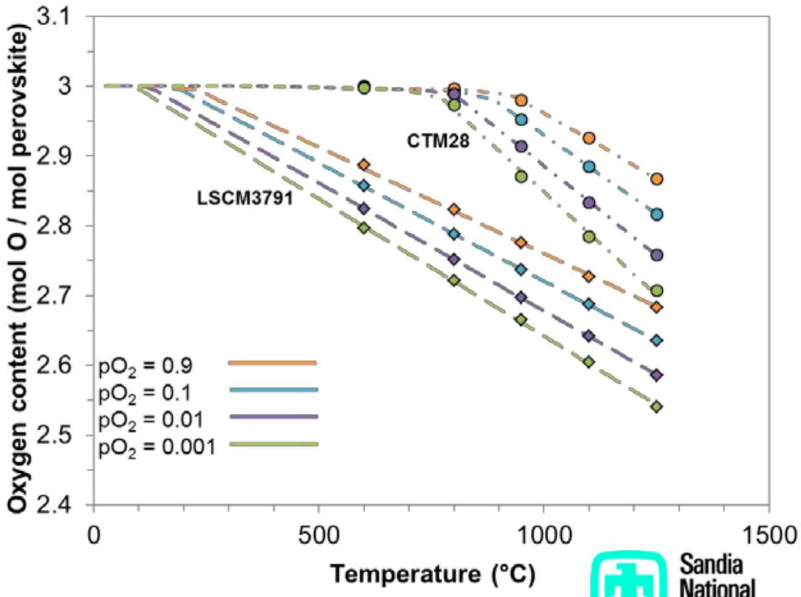

CAM28 Cyclic Behavior

Extended thermal redox cycling in TGA

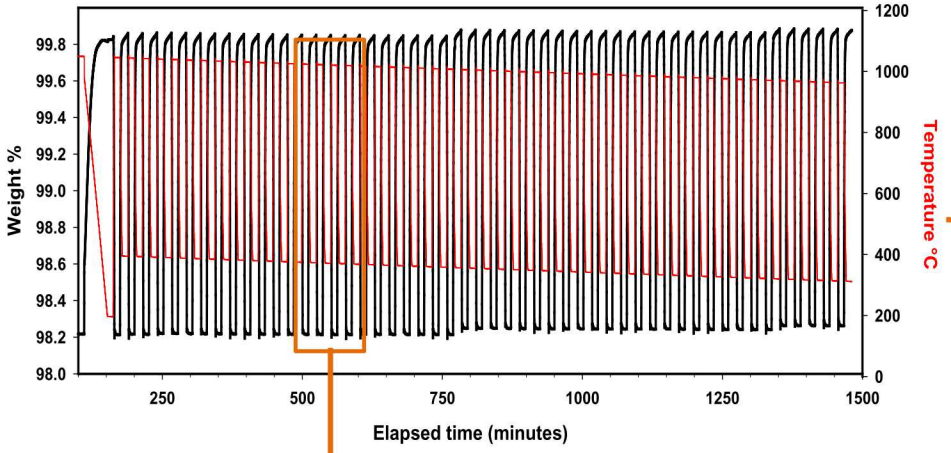

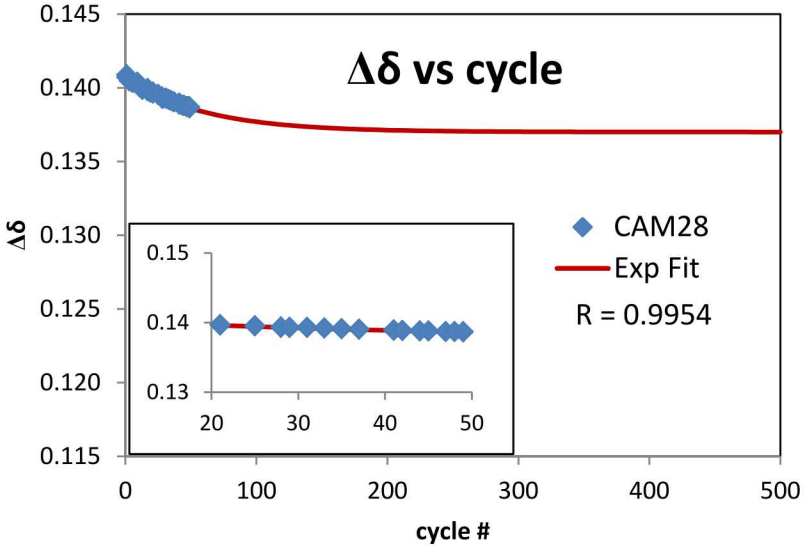

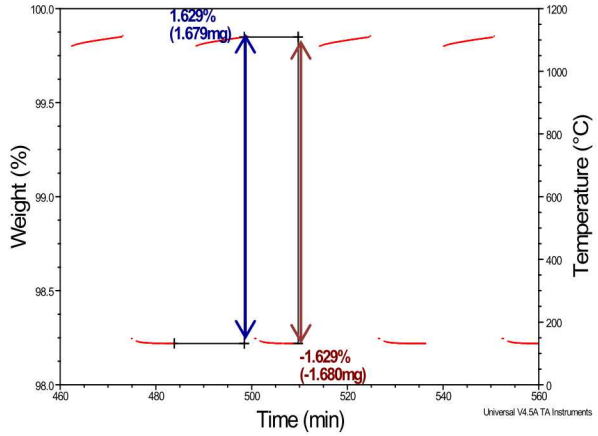

Before

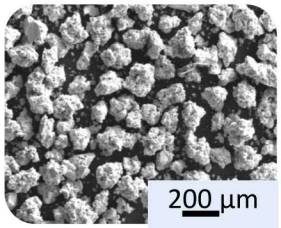

After

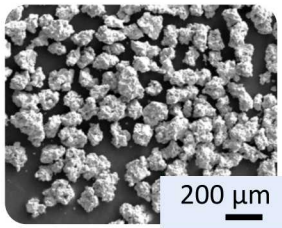

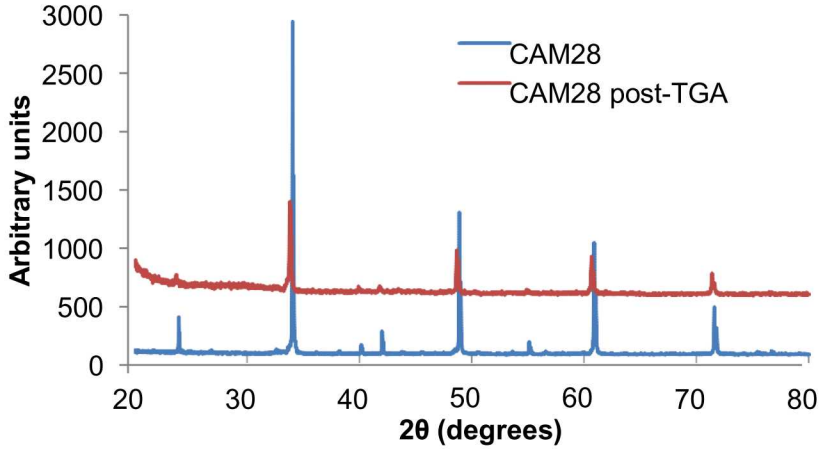

SEM of cycled particles

SunShot U.S. Department of Energy

Sandia National Laboratories

Y-Doped $CaMnO_3$

CYM28

- Analogue of CAM28
- Large increase of T_{red} - 1022 °C in air
- Not single phase
- Poor redox capacity
- Y seems to substitute on the A-site (for Ca) rather than on the B-site
  - Increase in T_{red} observed in other A-site doped $CaMnO_3$ compositions
  - *Can A-site doping result in an increased T_{red} while maintaining the higher redox properties of the parent compound?*

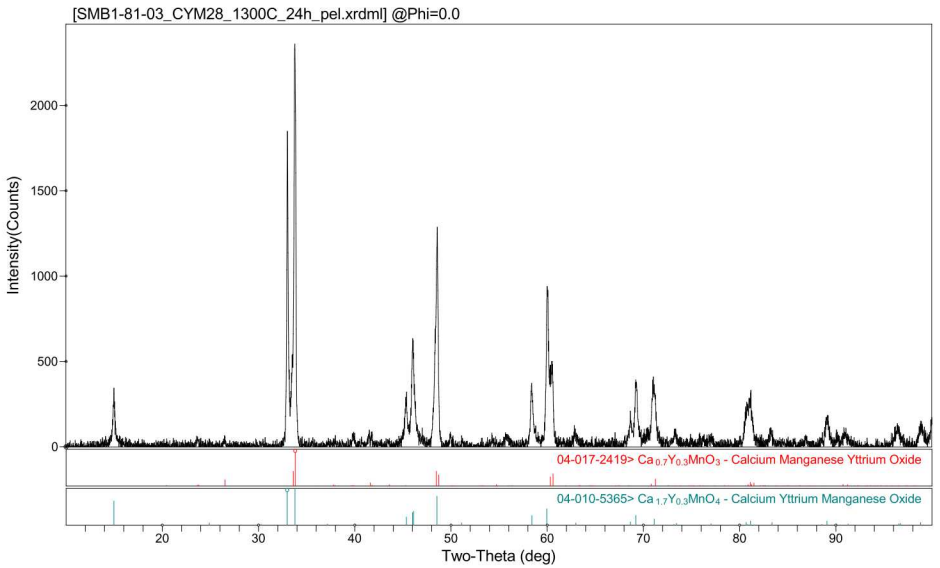

$Ca_{0.7}Y_{0.3}MnO_3$ orthorhombic
$Ca_{1.7}Y_{0.3}MnO_4$ tetragonal

$Ca_{1-x}Y_xMnO_3$ (0<x<0.5)

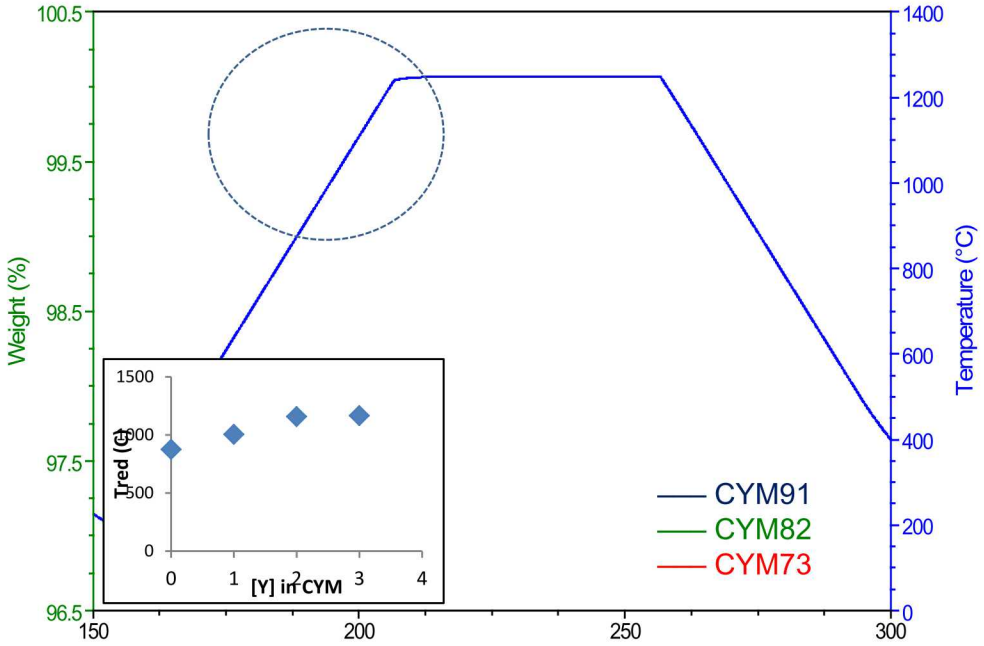

- Balance between T_{red} and reduction extent (δ)
- At what point does T_{red} become too high?

- T_{red} increases with increasing [Y]
- Corresponding δ decreases with increasing [Y]

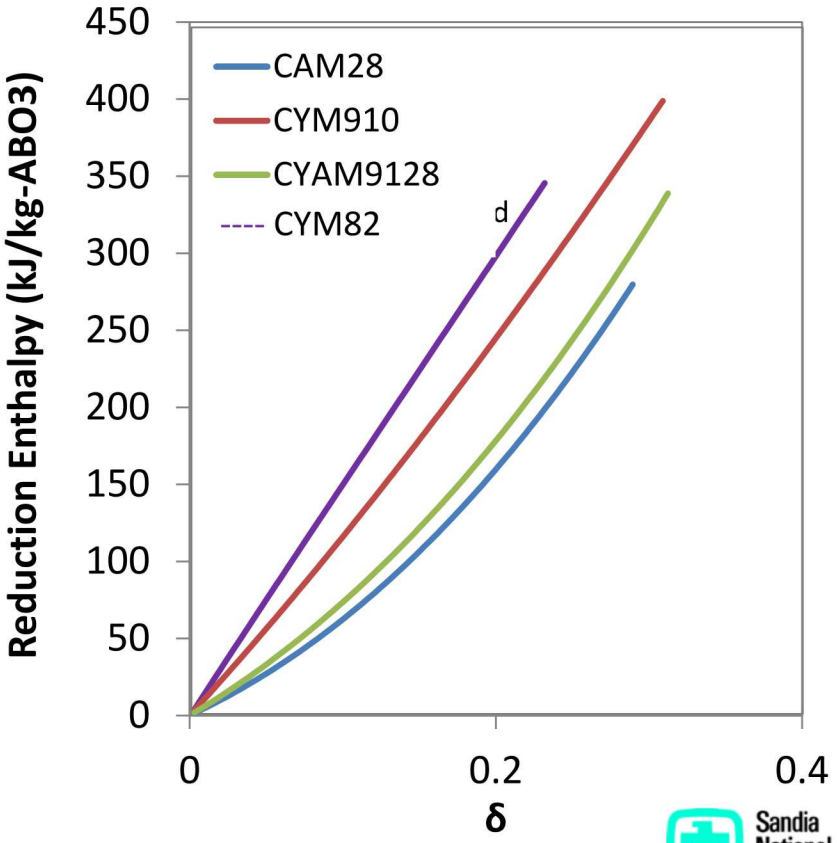

Conclusions

- Initial LSCX investigation provided insight on structural/thermal properties of TCES perovskites
  - Promising ΔH_{total} values achieved, but reduction extent is adequate, but reaction enthalpy falls short of 1500 kJ/kg goal
- Reduction onset temperature (T_{red}) was identified as a key indicator of ΔH_{rxn}
- $CaMnO_3$ displays high T_{red} but decomposes under reducing conditions
- B-site doping with non-labile cations (Al, Ti) mitigates decomposition while maintaining redox properties
  - ΔH_{total} approaching1500 kJ/kg
  - Increase in reaction enthalpy of over 50% compared to LSXM
  - *To our knowledge these materials outperform any reported oxide TCES material operating above 1000 °C*
- A-site doping with Y further increases T_{red}
  - Sacrifice redox extent
  - What is the ideal balance between T_{red} and δ?
- Judicious choice of A- and B- sited dopants in $CaMnO_3$ can result in effective TCES materials across a wide range of operating parameters

PROMOTES

Related Talks

- James Miller, "High Performance Reduction/Oxidation Metal Oxides for Thermochemical Energy Storage (PROMOTES)", Wednesday, Session 2-8-9
- Ellen Stechel, "Model-Free Thermodynamic Relationships for Non-Stoichiometric Metal Oxides (MO_{x-d}) from d-Temperature-pO2 Experimental Measurements", Wednesday, Session 2-6-1
- Robert Gill, "Solar Electricity via an Air Brayton Cycle with an Integrated Two-Step Thermochemical Cycle for Heat Storage Based on Non-Stoichiometric $CaAl_{0.2}Mn_{0.8}O_{3-d}$ Redox Reactions: Kinetic Analysis", Thursday, Session 2-6-3
- Sean Babiniec, "Considerations for the Design of a High-Temperature Particle Reoxidation Reactor for Heat Extraction in Thermochemical Energy Storage Systems", Thursday, Session 2-8-11

Thank you for your attention. Questions?

SunShot U.S. Department of Energy

Sandia National Laboratories

Backup Slides

PROMOTES

High Performance Reduction/Oxidation Metal Oxides for Thermochemical Energy Storage

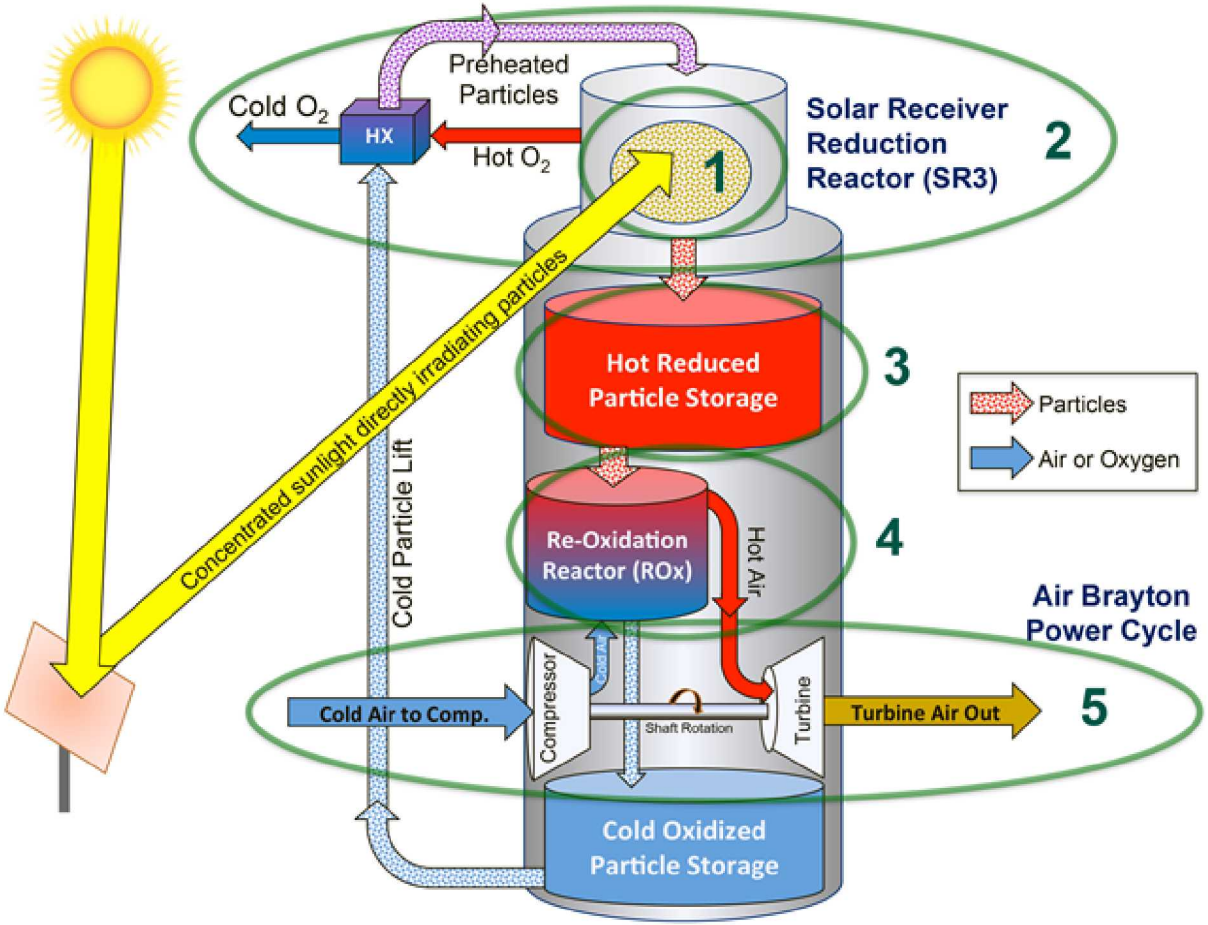

1. Materials Enabled Innovation ($\Delta H_{total} \geq 1500$ kJ/kg)
2. Solar Receiver Reduction Reactor
3. Particle Storage at T > 1000 ºC
4. Pressurized oxidation reactor Air acts as reactant and heat transfer fluid. Open cycle – no gas storage.
5. High Temp/High Efficiency Air Brayton Power Cycle.

Characterization-TGA

Preliminary Screening

- Used to determine potential redox properties quickly
- Materials are not at equilibrium
- More involved equilibrium TGA measurements performed on samples that meet criteria ($\Delta\delta \geq 0.2$)

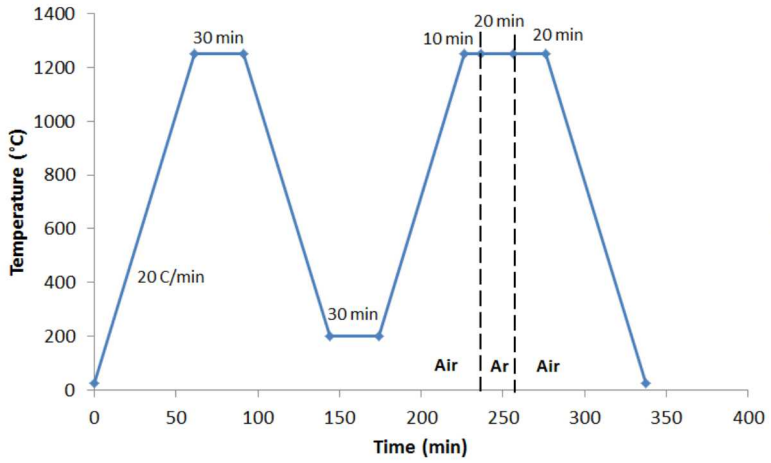

Pre-screen method

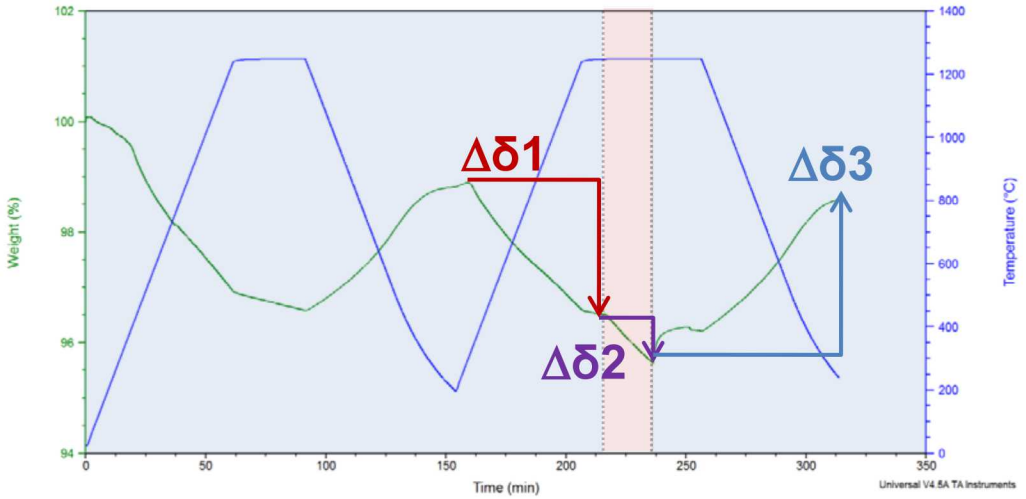

Example TGA

Measured weight changes are categorized in three regions:

- $\Delta\delta 1$: reduction in air from 200 to 1250 °C
- $\Delta\delta 2$: reduction due Ar switch at 1250 °C
- $\Delta\delta 3$: reoxidation due to air gas switch at 1250 °C and cooling to 200 °C

Materials: Reaction Enthalpy

$$ABO_3 + \Delta H_{rxn} \leftrightarrow ABO_{3-\delta} + \delta/2\ O_2(g)$$

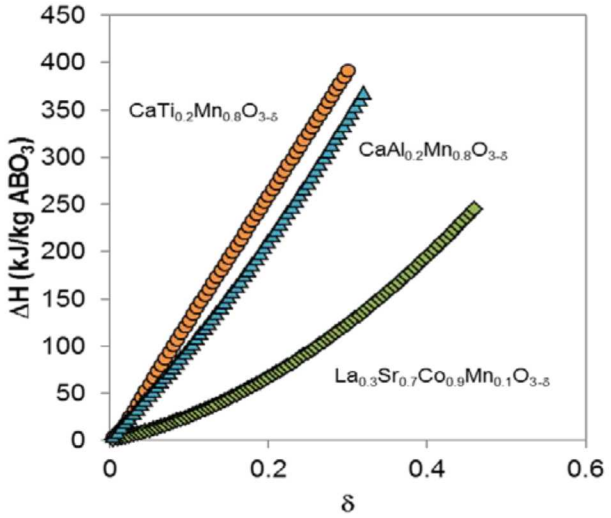

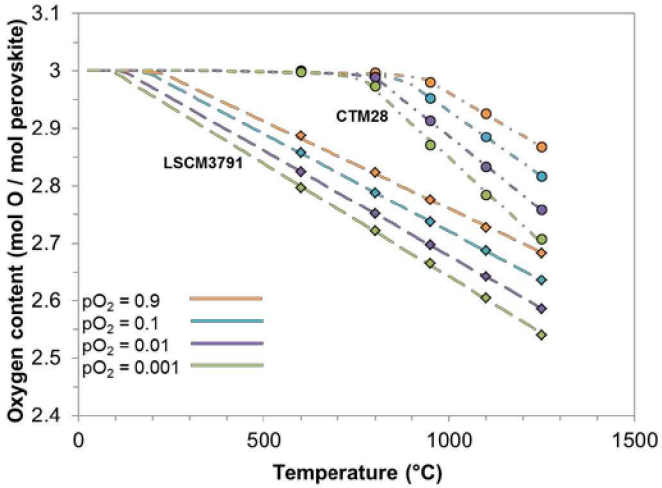

- First generation: Investigated/characterized LSCM, LSCF, and related perovskite families to identify baseline composition, LSCM3891, with high redox capacity (δ = 0.46) and reasonable ΔH_{rxn} (242 kg/kJ)
- Second generation: Low-cost earth-abundant compositions CXM (X = Ti, Al)
  - Lower redox capacity compensated by higher T_{red} → Stronger M-O bonds and storage of higher-quality heat
  - Smaller molecular weight results in higher specific heat, and therefore mass-specific total enthalpy

Materials: Total Storage Capacity

$$\Delta H_{tot} = \Delta H_{rxn} + C_p \Delta T$$

Chemical + Sensible Energy Storage

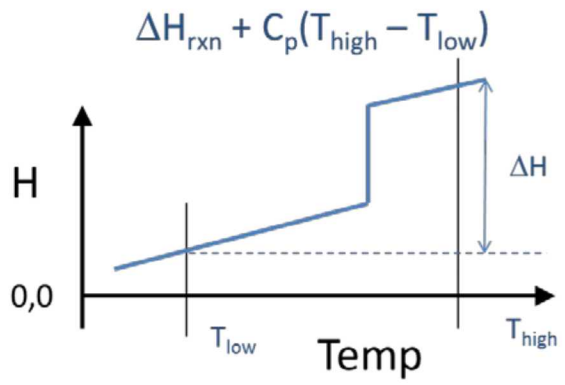

Measured heat capacity as a function of temperature

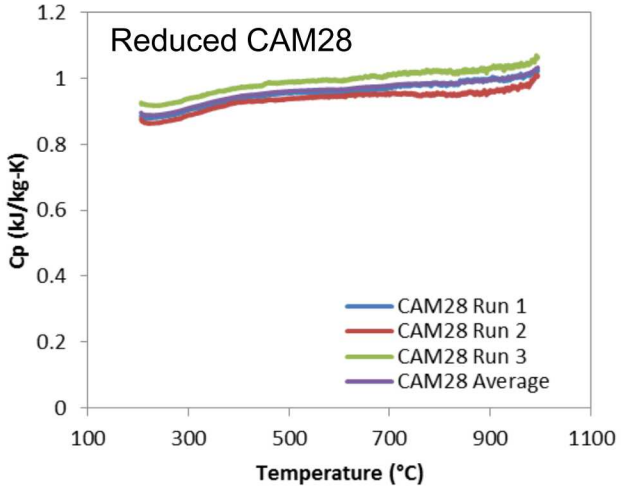

Candidate material	Mol weight (g/mol)	T_{red} Onset (°C)	Max δ	ΔH_{rxn} (kJ/kg) (at δ_{max})	C_p (kJ/kg-K)	ΔH_{tot} (kJ/kg)
LSCM3791	209.5	343	0.461	242	*0.595	837
CTM28	141.6	901	0.293	393	*0.881	1274
CAM28	135.8	759	0.322	371	*0.910	1281

*Estimated Values: C_p = 3R·N (J/mol-K) = 15R, T_{high} = 1200 °C, T_{low} = 200 °C

Doped CMO Screening

Calcium perovskites exhibit higher reduction temperatures than LSCM/LSCF

Composition	>95% Single-phase?	Crystal structure	Reduction onset in air (°C)	Δδ
$CaMnO_{3-\delta}$ (CM)	Yes	Orthorhombic	875	0.27
$CaTi_{0.2}Mn_{0.8}O_{3-\delta}$ (CTM28)	Yes	Orthorhombic	901	0.21
$CaTi_{0.4}Mn_{0.6}O_{3-\delta}$ (CTM46)	Yes	Orthorhombic	992	0.13
$Ca_{0.8}La_{0.2}Ti_{0.4}Mn_{0.6}O_{3-\delta}$ (CLTM8228)	Yes	Orthorhombic	1020	0.09
$Ca_{0.8}Sr_{0.2}Ti_{0.4}Mn_{0.6}O_{3-\delta}$ (CSTM8228)	Yes	Orthorhombic	827	0.24
$CaCo_{0.2}Mn_{0.8}O_{3-\delta}$ (CCM28)	Yes	Orthorhombic	730	0.27
$CaFe_{0.2}Mn_{0.8}O_{3-\delta}$ (CFM28)	Yes	Orthorhombic	418	0.28
$CaFe_{0.4}Mn_{0.6}O_{3-\delta}$ (CFM46)	Yes	Orthorhombic	427	0.24
$CaAl_{0.2}Mn_{0.8}O_{3-\delta}$ (CAM28)	Yes	Orthorhombic	759	0.27

Prescreen profile for CAM28

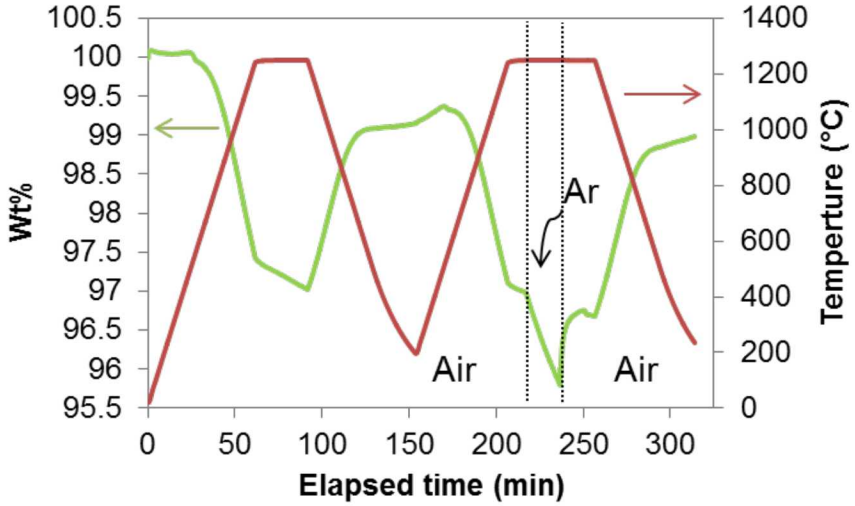

SunShot U.S. Department of Energy

Sandia National Laboratories

Subtask 2.1.1: CXM composition refinement

- Effort to optimize enthalpy in $CaX_xMn_{1-x}O_{3-\delta}$ (CXM)-based materials by balancing redox capacity with T_{red}:

(1) Vary X cation (Y, Zr, Zn) in CXM28
(2) A-site doping by La
(3) Vary [Ti] in CTM composition

Composition	Single Phase?	Reduction T (°C in air)	δ1	δ2	δ3
$CaAl_{0.2}Mn_{0.8}O_3$ (CAM28)	Y	760	0.20	0.10	0.27
$CaTi_{0.2}Mn_{0.8}O_3$ (CTM28)	Y	901	0.15	0.11	0.21
$Ca_{0.5}La_{0.5}Ti_{0.5}Mn_{0.5}O_3$ (CLTM5555)	Y	970	0.02	0.04	0.03
$CaTi_{0.6}Mn_{0.4}O_3$ (CTM64)	Y	951	0.06	0.08	0.10
$CaTi_{0.05}Mn_{0.95}O_3$ (CTM0595)	Y	843	0.21	0.13	0.29
$CaZn_{0.2}Mn_{0.8}O_3$ (CZnM28)	N	872	0.13	0.10	0.20
$CaZr_{0.2}Mn_{0.8}O_3$ (CZrM28)	N	867	0.17	0.10	0.24
$CaY_{0.2}Mn_{0.8}O_3$ (CYM28)	N	1022	0.03	0.07	0.07

Preliminary TGA screening properties for newly-synthesized compositions. CAM28 and CTM28 are added for reference. Candidate compositions are highlighted.

Phase Determination

All synthesized doped calcium perovskites indexed to the orthorhombic phase

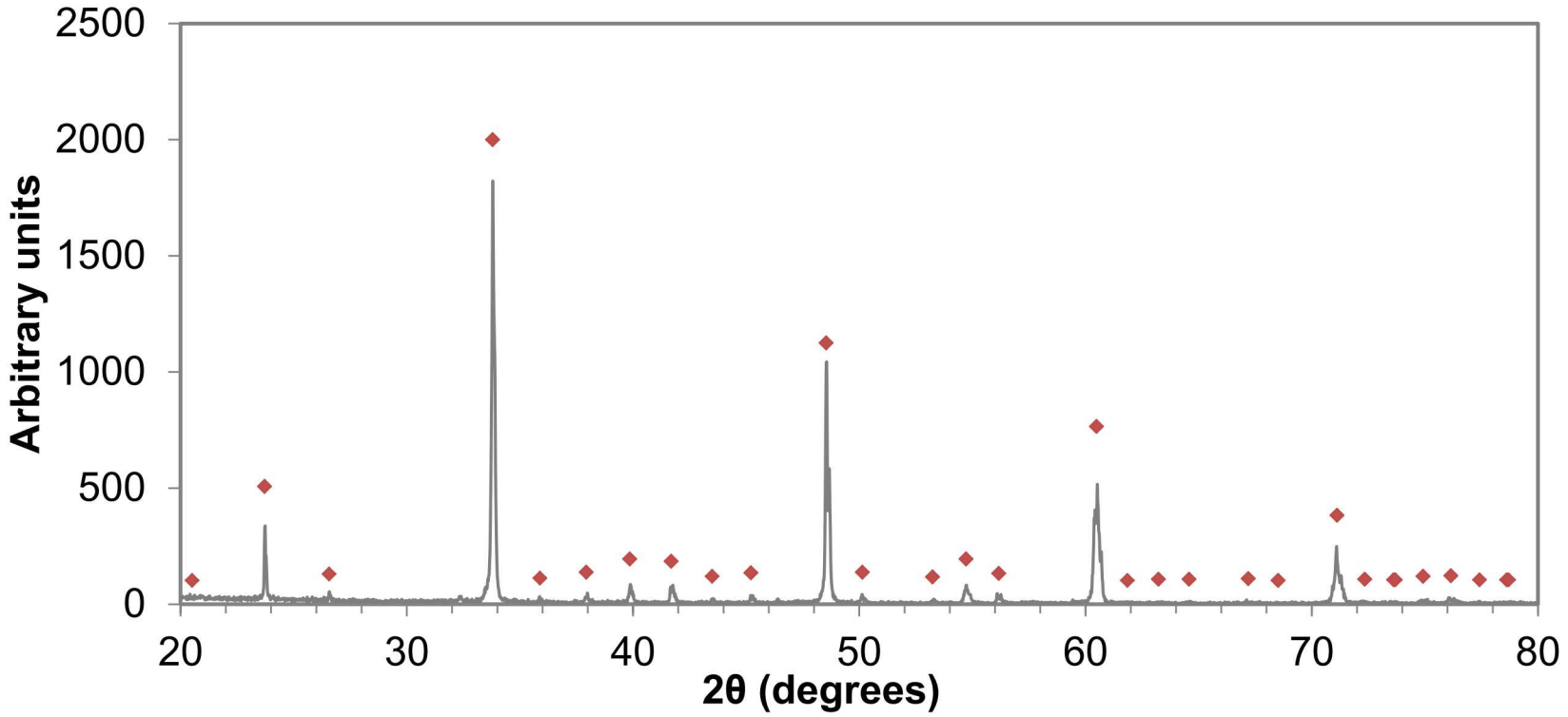

CTM28 XRD indexed to orthorhombic perovskite phase (red symbols), PDF#01-070-7307

T_{red} vs [Y]

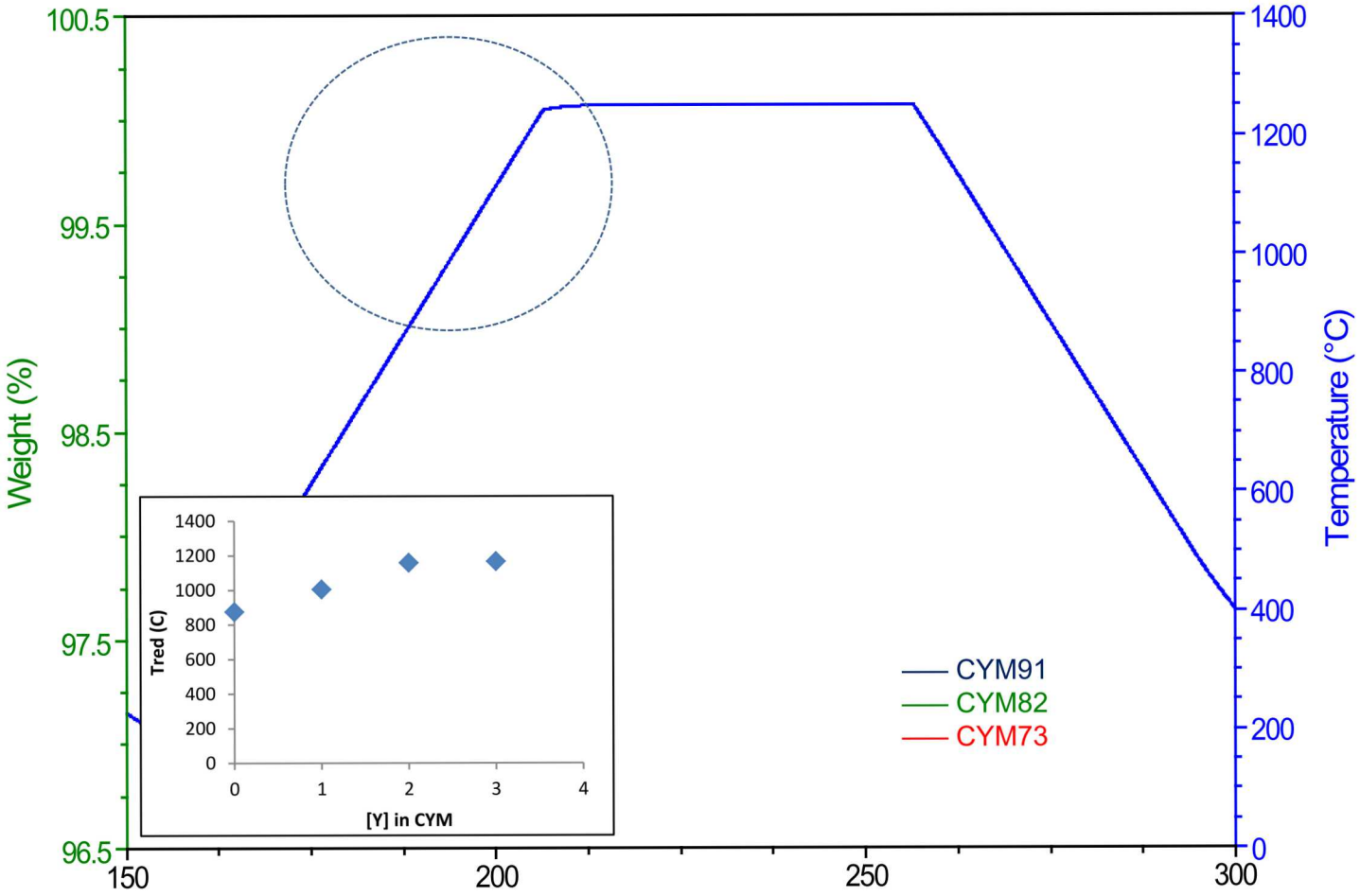
100.5
99.5
98.5
97.5
96.5
Weight (%)
150
200
250
300
1400
1200
1000
800
600
400
200
0
Temperature (°C)
CYM91
CYM82
CYM73
Tred (C)
[Y] in CYM
0
1
2
3
4

Lattice Distortion

X-ray diffraction shows peak splitting in CYM910

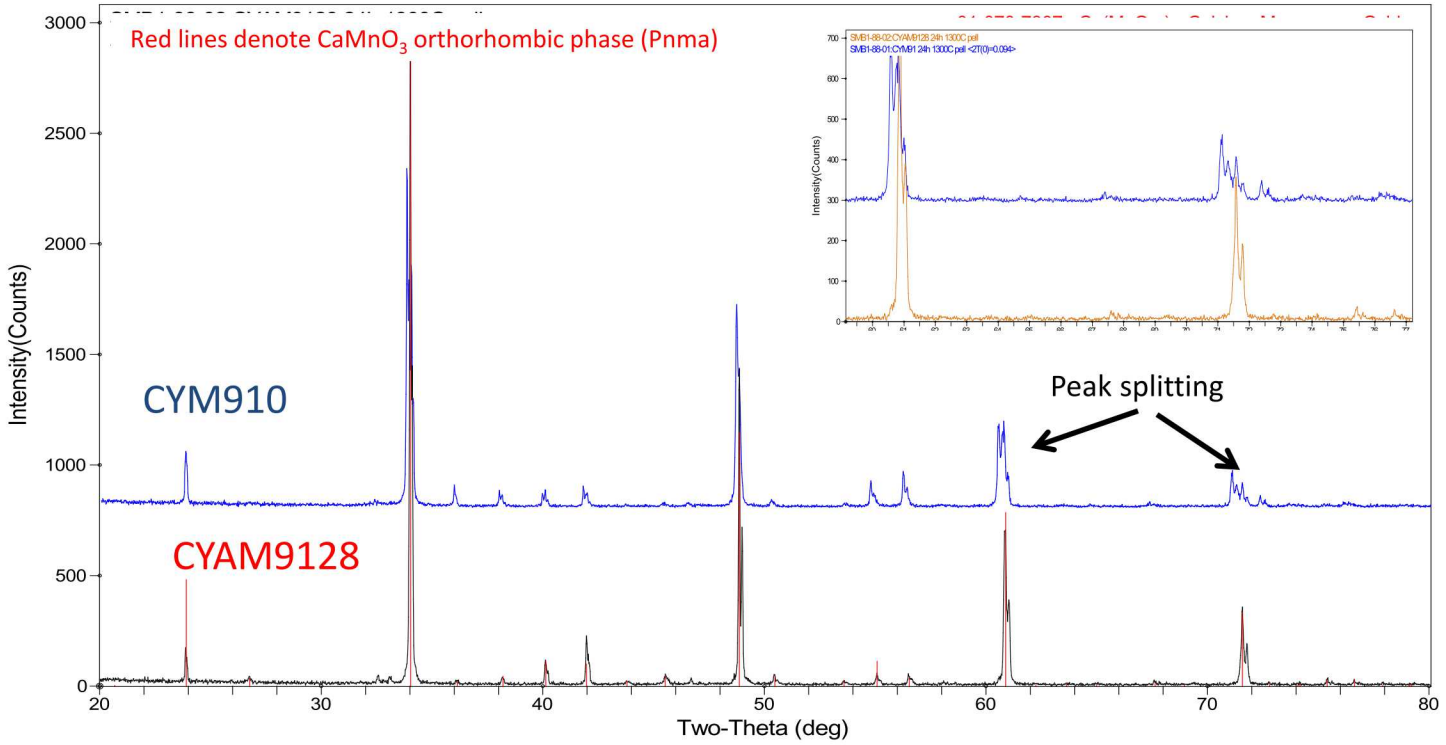

- Likely due to oxygen vacancy ordering (as reported in $CaMnO_{2.5}$) or octahedral distortion from Y-doping
- CYAM9128 does not distort – possibly stabilized by B-site Al
- Could order/disorder result in increased enthalpy?

Y-doped Compositions

Material	MW (g/mol)	Single Phase?	δ1	δ2	δ3	T_{red} (°C)
$CaMnO_3$	143.0	Y	0.224	0.127	0.315	875
$CaAl_{0.2}Mn_{0.8}O_{2.9}$ (CAM28)	135.8	Y	0.203	0.100	0.270	759
$Ca_{0.9}Y_{0.1}Al_{0.2}Mn_{0.8}O_3$ (CYAM9128)	142.3	Y	0.204	0.101	0.288	800
$Ca_{0.9}Y_{0.1}MnO_3$ (CYM910)	147.9	Y	0.159	0.116	0.251	966
$Ca_{0.8}Y_{0.2}MnO_3$ (CYM820)	152.9	Y	0.106	0.0724	0.175	1158

- T_{red} increases with increasing [Y]
- Corresponding δ decreases with increasing [Y]

Reduction Extent

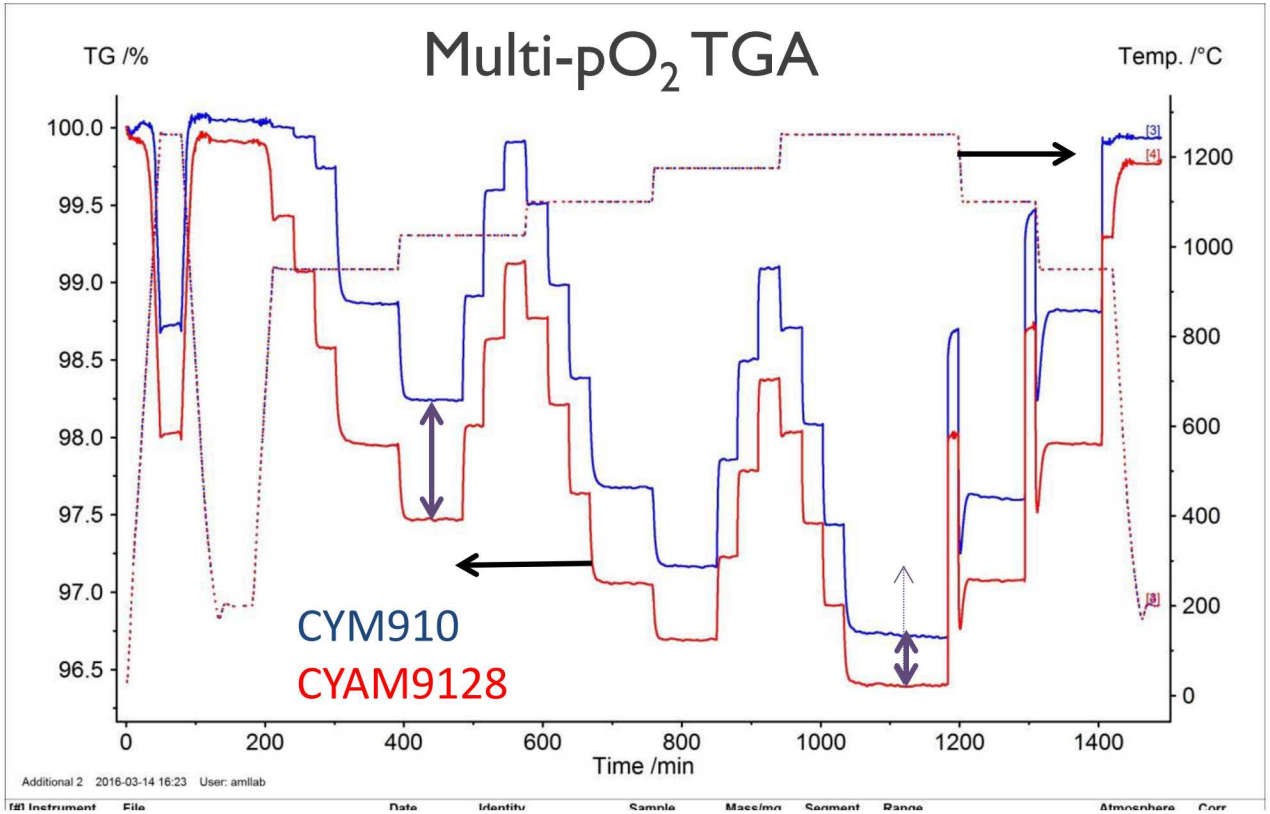

- Difference in reduction extent between CYM and CYAM larger at low-T, but begins to converge as reduction T increases
- CYM experiences larger magnitude of reduction at high T
- Indicates stronger M-O bonds and storage of higher-quality heat resulting in increased ΔH_{rxn}